



Dyna

ISSN: 0012-7353

dyna@unalmed.edu.co

Universidad Nacional de Colombia

Colombia

Álvarez-Fernández, Martina Inmaculada; González-Nicieza, Celestino; Prendes-Gero, María Belén; García-Menéndez, José Ramón; Peñas-Espinosa, Juan Carlos; Suárez-Domínguez, Francisco José

Numerical analysis of the influence of sample stiffness and plate shape in the Brazilian test

Dyna, vol. 82, núm. 194, diciembre, 2015, pp. 79-85

Universidad Nacional de Colombia

Medellín, Colombia

Available in: <http://www.redalyc.org/articulo.oa?id=49643211011>

- How to cite
- Complete issue
- More information about this article
- Journal's homepage in redalyc.org

redalyc.org

Scientific Information System

Network of Scientific Journals from Latin America, the Caribbean, Spain and Portugal

Non-profit academic project, developed under the open access initiative

Numerical analysis of the influence of sample stiffness and plate shape in the Brazilian test

Martina Inmaculada Álvarez-Fernández ^a, Celestino González-Nicieza ^b, María Belén Prendes-Gero ^c, José Ramón García-Menéndez ^d, Juan Carlos Peñas-Espinosa ^e & Francisco José Suárez-Domínguez ^f

^a Departamento de Explotación y Prospección de Minas, Universidad de Oviedo, Oviedo, Asturias, España. inma@git.uniovi.es

^b Departamento de Explotación y Prospección de Minas, Universidad de Oviedo, Oviedo, Asturias, España. celes@git.uniovi.es

^c Departamento de Construcción e Ingeniería de Fabricación, Universidad de Oviedo, Gijón, Asturias, España. belen@git.uniovi.es

^d Departamento de Explotación y Prospección de Minas, Universidad de Oviedo, Oviedo, Asturias, España. juan@git.uniovi.es

^e Departamento de Explotación y Prospección de Minas, Universidad de Oviedo, Oviedo, Asturias, España. penasjc@ocacp.es

^f Departamento de Construcción e Ingeniería de Fabricación, Universidad de Oviedo, Gijón, Asturias, España. paco@constru.uniovi.es

Received: September 19th, 2014. Received in revised form: August 6th, 2015. Accepted: September 24th, 2015.

Abstract

Due to the heterogeneity of rocks, their tensile strength is around 10% of their compressive strength, which means that breakage is mainly caused by tensile stress. The measure of tensile stress is very difficult due to rock fragility, so it has usually been measured by indirect measurement methods, including the Brazilian test. However, recent works indicate that the tensile strength values obtained through the Brazilian test must be increased by almost 26%.

To understand this divergence, indirect tensile tests have been monitored. The aim is to know the material deformation and load increase by means of stepwise regression. Stress fields in slightly deformed samples are analyzed and modeled (3D finite differences) with loads applied on flat and curved plates and different Young's modulus. Finally, the results are analyzed and compared with strength values reported using Timoshenko theory and Hondros' approximation.

Keywords: Brazilian test; test monitoring; numerical simulation.

Análisis numérico de la influencia de la dureza de la muestra y la forma de placa en el ensayo Brasileño

Resumen

La heterogeneidad de las rocas hace que su fuerza tensora sea un 10% de su fuerza de compresión provocando roturas principalmente por tensión. Sin embargo la resistencia a tensión es muy difícil de medir debido a la fragilidad de la roca, por lo que normalmente se emplean métodos de medida indirecta entre los que destaca el ensayo Brasileño. Sin embargo trabajos recientes indican que este ensayo reduce en un 26% los valores de resistencia.

Para entender esta divergencia, se han monitorizado ensayos de tensión indirecta. El objetivo es conocer la deformación del material y la carga discontinua incrementada. Se han analizado y modelado los campos de tensión de muestras ligeramente deformadas mediante cargas aplicadas en platos curvos y planos y con diferentes Módulos de Young. Los resultados se analizan y comparan con los valores obtenidos con la Teoría de Timoshenko y la Aproximación de Hondros.

Palabras clave: Ensayo Brasileño; ensayo de monitorización; simulación numérica.

1. Introduction

Rocks and artificial materials are not generally homogeneous and contain numerous micro-cracks, show anisotropy and grain-matrix resistance differences, this

meaning that the tensile strength is lower than the compressive strength. Most of the efforts have been focused in calculate the compression strength of the materials [1,2], but rock breakage is mainly due to its low tensile strength (approximately 10% of its compressive strength).

Great efforts have been focused on determining rock tensile strength. However, due to rock fragility, no direct tensile tests can be completed, so techniques developed until now have always been focused on the development of indirect measurement methods.

In 1971 Mellor & Hawkes [3] thoroughly researched the Brazilian test, also known as the diametrical compressive test. As a result, they presented a formula that allows rock tensile strength to be calculated. Several years later, the International Society of Rocks Mechanics (ISRM), proposed that the Brazilian test be made the standard method to determine rock tensile strength [4]. Due to the ease of its implementation, this method has been widely adopted in many fields and countries over the last 20 years. For instance, China included it among its engineering regulations in the 1980s [5], as well as in State regulations and specifications for water storage and hydroelectric power in 1999 and 2001 [6,7]. The Brazilian test, although with slight variations, is currently applied to measure tensile strength in concrete [8], rock materials [9], concrete and ceramic materials [10], pharmaceutical materials [11], and other fragile materials.

For the tensile test, a testing sample extracted from the material to be analyzed is used. This sample can be of either disc or cube-shaped; however, the disc-shaped type is more widely used since probes are easy to obtain and it demands almost no mechanizing. According to the literature [3-7], the disc diameter usually ranges from 48 to 54 mm, and the disc thickness-radius ratio ranges from 0.5 mm to 1 cm.

Some researchers have recently completed works on the Brazilian test [12], proposing new formulae to estimate tensile strength, starting with the formula contributed by Timoshenko & Goodier [13]. Yong et al. [14] and Yong et al. [15] completed their correction of the test by maximizing the initial expression with a coefficient which, in the first work, depends on disc shape and dimensions and, in the second, depends on the sample's Poisson coefficient. In both cases, the coefficient is obtained by numerical simulations with finite 3D elements. The result is increase of over 26% and 30%, respectively. Jonsen et al. [16] obtain 25% higher tensile results. These authors consider experimental methods and fracture energy in compressed materials (pressed metal powders). Other authors such as Jianhong et al. [17] make an estimate for the rock tensile elastic module and propose a formula based on the tensile strength in rocks obtained from the Brazilian test. Es-Saheb et al. [18] analyze, by means of finite elements, the influence of materials such as flat grounds and soft pads on stress distribution. It seems clear that the current trend considers a higher tensile strength value than that obtained with the Brazilian test.

To be able to understand variation in tensile strength values and, more precisely, the tendency that started last years to consider values over 20% of those obtained in Brazilian tests, numerous indirect tensile tests have been monitored. This monitoring is aimed at observing how materials deform throughout time and under increasing loading values. Once this behavior is analyzed, the values are calculated and modeled by means of 3D finite differences with loads applied on flat and curved plates and with varying Young's modulus. Finally, results are analyzed and compared to the strengths obtained with the Timoshenko theory and Hondros' approximation.

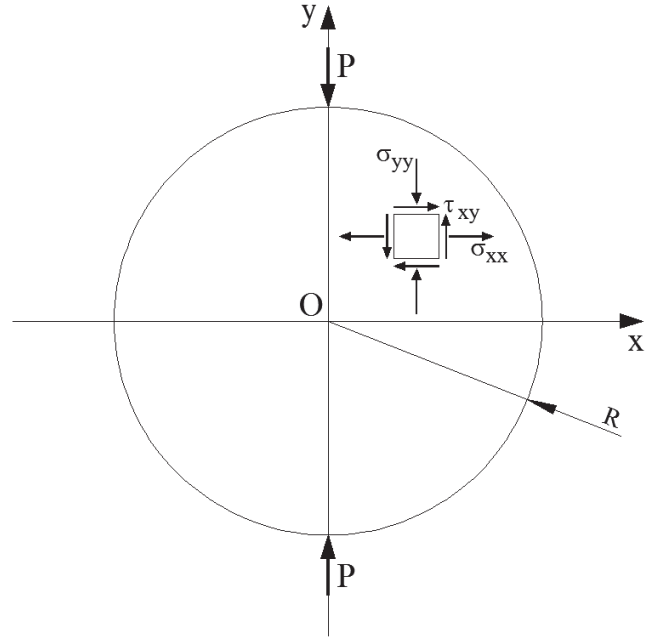


Figure 1. Test of diametrical compression by “points” loads.
Source: Álvarez Fernández et al.

2. Methods

2.1. Stress fields in diametrical compression by “points” loads

Diametrical compression by “points” loads involves a tensile stress perpendicularly to the compressed diameter which depending on the theory followed- holds sensitively constant in a wide-enough area of the disc center [8,11]. Under these conditions and applying Timoshenko theory, the stress fields at all points in a disc with radius R , thickness t , and subjected to actual loads of magnitude P in extreme points within the same diameter (Fig. 1) [13,19] are given by:

$$\begin{cases} \sigma_{xx}(x, y) = Q \left[\frac{1}{2R} - x^2 (R_1^*(x, y) + R_2^*(x, y)) \right] \\ \sigma_{yy}(x, y) = Q \left[\frac{1}{2R} - (R - y)^2 R_1^*(x, y) - (R + y)^2 R_2^*(x, y) \right] \\ \tau_{xy}(x, y) = Qx \left[(R - y) R_1^*(x, y) - (R + y) R_2^*(x, y) \right] \end{cases} \quad (1)$$

Where:

$$\begin{aligned} Q &= \frac{2P}{\pi t} \\ R_1^*(x, y) &= \frac{R - y}{[x^2 + (R - y)^2]^2} \\ R_2^*(x, y) &= \frac{R + y}{[x^2 + (R + y)^2]^2} \end{aligned} \quad (2)$$

Eq. (1) allows for stresses to be obtained n along axes x eq. (3) and y eq. (4) by annulling variable y or x, respectively.

$$\begin{cases} \sigma_{xx}(x,0) = Q \left[\frac{1}{2R} - \frac{2x^2 R}{(x^2 + R^2)^2} \right] \\ \sigma_{yy}(x,0) = Q \left[\frac{1}{2R} - \frac{2R^3}{(x^2 + R^2)^2} \right] \\ \tau_{xy}(x,0) = 0 \end{cases} \quad (3)$$

$$\begin{cases} \sigma_{xx}(0,y) = \frac{Q}{2R} = \frac{P}{\pi R t} \\ \sigma_{yy}(0,y) = Q \left[\frac{1}{2R} - \frac{2R}{R^2 - y^2} \right] \\ \tau_{xy}(0,y) = 0 \end{cases} \quad (4)$$

In eq. (4), the horizontal stress is deduced to be constant along the vertical diameter and vertical line to tend to infinite in the extreme points of the diameter. Likewise, in eq. (1), the strengths at the disc center can be deduced equaling variables x and y to zero:

$$\sigma_{xx}(0,0) = \frac{P}{\pi R t}; \quad \sigma_{yy}(0,0) = -\frac{3P}{\pi R t} = -3\sigma_{xx} \quad (5)$$

Disc center stresses eq. (5) show that upon breakage, vertical compressive stress is three times higher than horizontal tensile stress. If the Mohr's circle corresponding to this stress state is drawn, and considering that breakage occurs at the point of the circle tangent which is on the envelope of Fig. 2, an error in estimating the tensile strength would be made. This error would be around 40%, but yes, the side of safety.

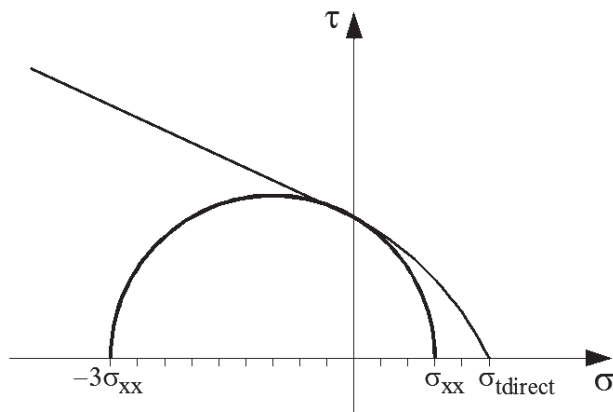


Figure 2. Tensile breakage in the Brazilian test.
Source: Álvarez Fernández et al.

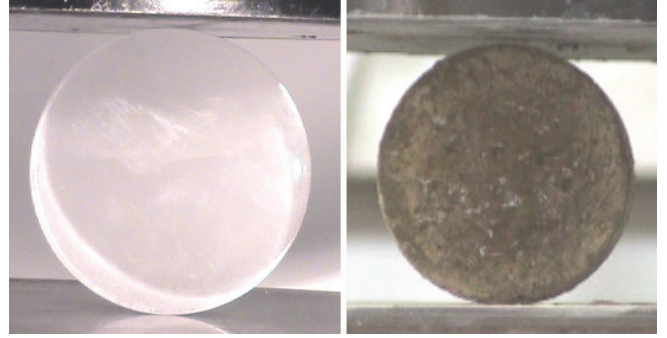


Figure 3. Tensile test monitoring: onset.
Source: Álvarez Fernández et al.

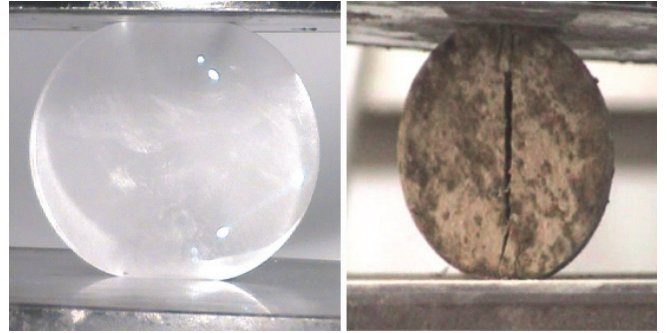


Figure 4. Tensile test monitoring: deformation throughout time.
Source: Álvarez Fernández et al.

To understand what happens in an indirect stepwise tensile test, numerous indirect tensile tests have been monitored. 50 mm diameter samples with approximately the same thickness as the sample radius were used in all tests and tensile stresses was applied at a speed of approximately 200 N/s [20].

Fig. 3 shows the onset of a test on methacrylate (left-hand) and concrete (right-hand) samples, while Fig. 4 shows deformation throughout time. The methacrylate test is not exactly a Brazilian test since it changes from tensile to simple compressive, yet this work is reported because it allows clear observation of the deformation process throughout time. These tests allow for it to be deduced that in the earliest moments of the test (Fig. 3), samples present linear contact with the machine's clamps along a generatrix. However, an increased applied load leads to sample deformation and transforms initially linear contact into superficial contact, that is until breakage occurs (Fig. 4).

Therefore, the initial linear diameter compressive defined by Timoshenko [11] occurs, and as time goes by and load increases, compression is applied on horizontal strips, similar to yet slightly different from Hondros' approximation [8]. This considers that contact occurs on 2α amplitude curved areas.

2.2. Field of compressive stresses by loads on diametrically opposed arches

The application of Hondros' theory gives rise to stress fields along the horizontal and vertical diameters, defined by eq. (6), (7), respectively Fig. 5.

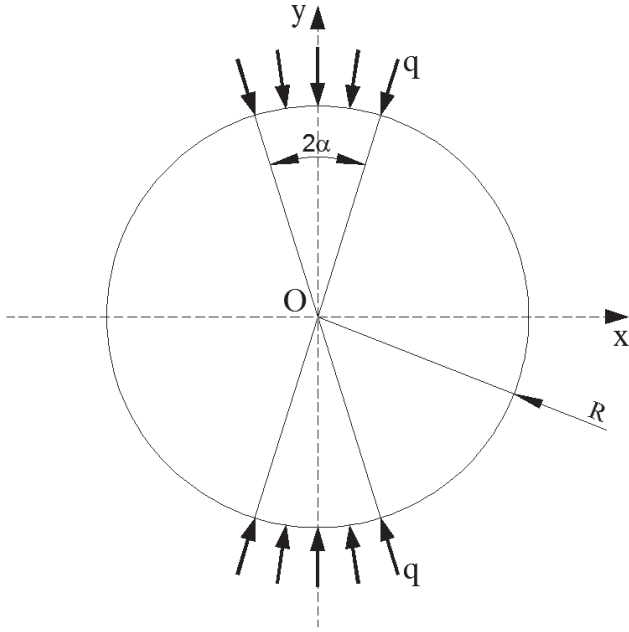


Figure 5. Compression on diametrically opposed arches.
Source: Álvarez Fernández et al.

$$\left\{ \begin{array}{l} \sigma_{xx}(x,0) = \frac{2q}{\pi} \left[\frac{\left(1 - \frac{x^2}{R^2}\right) \cdot \sin 2\alpha}{1 + \frac{2x^2}{R^2} \cos 2\alpha + \frac{x^4}{R^4}} - \arctg \left(\frac{1 - \frac{x^2}{R^2}}{1 + \frac{x^2}{R^2}} \cdot \tg \alpha \right) \right] \\ \sigma_{yy}(x,0) = -\frac{2q}{\pi} \left[\frac{\left(1 - \frac{x^2}{R^2}\right) \cdot \sin 2\alpha}{1 + \frac{2x^2}{R^2} \cos 2\alpha + \frac{x^4}{R^4}} + \arctg \left(\frac{1 - \frac{x^2}{R^2}}{1 + \frac{x^2}{R^2}} \cdot \tg \alpha \right) \right] \\ \tau_{xy}(x,0) = 0 \end{array} \right. \quad (6)$$

$$\left\{ \begin{array}{l} \sigma_{xx}(0,y) = \frac{2q}{\pi} \left[\frac{\left(1 - \frac{y^2}{R^2}\right) \cdot \sin 2\alpha}{1 - \frac{2y^2}{R^2} \cos 2\alpha + \frac{y^4}{R^4}} - \arctg \left(\frac{1 + \frac{y^2}{R^2}}{1 - \frac{y^2}{R^2}} \cdot \tg \alpha \right) \right] \\ \sigma_{yy}(0,y) = -\frac{2q}{\pi} \left[\frac{\left(1 - \frac{y^2}{R^2}\right) \cdot \sin 2\alpha}{1 - \frac{2y^2}{R^2} \cos 2\alpha + \frac{y^4}{R^4}} + \arctg \left(\frac{1 + \frac{y^2}{R^2}}{1 - \frac{y^2}{R^2}} \cdot \tg \alpha \right) \right] \\ \tau_{xy}(0,y) = 0 \end{array} \right. \quad (7)$$

In this case, compressive stress in the extreme points on the vertical axis is not infinite, as is true in the case of actual

loads, yet and similarly, maximum tensile stress is found at disc center, eq. 8.

$$\sigma_{xx}(0,0) = \frac{2q}{\pi} (\sin 2\alpha - \alpha) \quad (8)$$

The applied force P can be expressed as $P=q \cdot 2Rt$ and, small α values with maximum fracture strength coincide with what was obtained applying Timoshenko theory. Therefore, at the disc center, both Timoshenko's and Hondros' theories are equivalent. Strength calculation is completed on a non-deformed sample in both theories. However, tensile test monitoring Fig. 3 shows that the sample progressively deforms as time goes by and the load increases. Therefore, this load is not applied on a curved surface but on a slightly flat surface due to deformation.

2.3. Stress Fields in compression by loads on deformed surfaces

Analysis of the stress fields in compression on slightly curved surfaces was completed by means of numeric simulation by applying explicit finite differences using the Flac3D software package.

Studies were completed with flat and curved plates (Fig. 6) using a 50 mm diameter cylinder, thickness equal to radius, 2500 kg/m³ density, and 104N applied force. Young's modulus values that were applied ranged from a minimum of 0.3375 GPa up to maximum of 67.5 GPa, which allows the influence of rock stiffness on sample strengths to be analyzed.

Model geometry was divided into 36351 nodes, and 33920 areas, and each element was assigned a linear elastic behavior model. Sample press plate contact was simulated by means of the interface logic with a 10° friction (Fig. 7). The stress-deformational estate of the model was solved by consecutive approximations, by recalculating the distribution of stresses and deformations in each calculation stage. In each stage, the unbalanced forces in each node produced acceleration and displacement. These were limited by the adjoining nodes, thus force redistribution was produced.

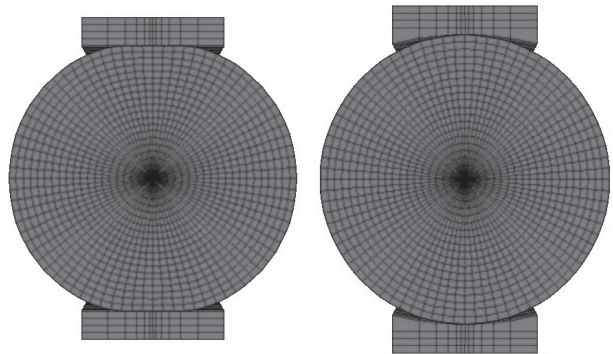


Figure 6. Plate shapes that were used.
Source: Álvarez Fernández et al.

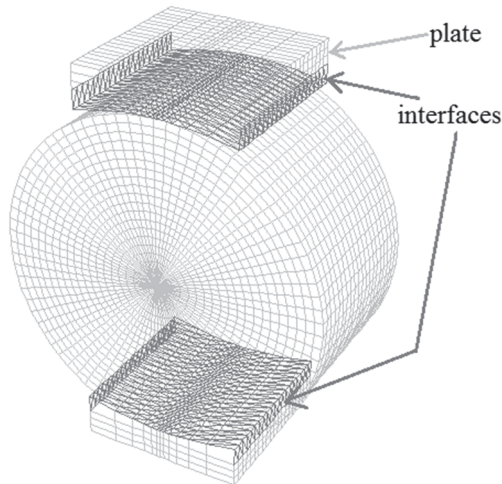


Figure 7. Geometry of calculus.
Source: Álvarez Fernández et al.

FLAC3D 3.00
Step 24000 Model Perspective
10:18:50 Wed Jun 05 2013

Center:	Rotation:
X: 0.000e+000	X: 0.000
Y: 1.250e-002	Y: 0.000
Z: 0.000e+000	Z: 0.000
Dist: 1.784e-001	Mag: 1
Increments:	Ang: 22.500
Move: 7.097e-003	Rot: 10.000

Contour of SXX
Magfac = 1.000e+000
Gradient Calculation

-2.8302e+007 to -2.8000e+007
-2.6000e+007 to -2.5000e+007
-2.3000e+007 to -2.2000e+007
-2.0000e+007 to -1.9000e+007
-1.7000e+007 to -1.6000e+007
-1.4000e+007 to -1.3000e+007
-1.1000e+007 to -1.0000e+007
-8.0000e+006 to -7.0000e+006
-5.0000e+006 to -4.0000e+006
-2.0000e+006 to -1.0000e+006
1.0000e+006 to 2.0000e+006
4.0000e+006 to 5.0000e+006
5.0000e+006 to 5.3500e+006

Interval = 1.0e+006

FLAC3D 3.00
Step 5000 Model Perspective
10:14:54 Wed Jun 05 2013

Center:	Rotation:
X: 0.000e+000	X: 0.000
Y: 1.250e-002	Y: 0.000
Z: 0.000e+000	Z: 0.000
Dist: 1.784e-001	Mag: 1
Increments:	Ang: 22.500
Move: 7.097e-003	Rot: 10.000

Contour of SXX
Magfac = 1.000e+000
Gradient Calculation

-4.4965e+007 to -4.4000e+007
-4.1000e+007 to -4.0000e+007
-3.7000e+007 to -3.6000e+007
-3.3000e+007 to -3.2000e+007
-2.9000e+007 to -2.8000e+007
-2.5000e+007 to -2.4000e+007
-2.1000e+007 to -2.0000e+007
-1.7000e+007 to -1.6000e+007
-1.3000e+007 to -1.2000e+007
-9.0000e+006 to -8.0000e+006
-5.0000e+006 to -4.0000e+006
-1.0000e+006 to 0.0000e+000
3.0000e+006 to 4.0000e+006
5.0000e+006 to 5.7650e+006

Interval = 1.0e+006

Figure 8. Horizontal stress with flat (upper) and curved (lower) plates.
Source: Álvarez Fernández et al.

The representation of the field of horizontal stresses for a sample of 6.75 GPa of stiffness (Fig. 8) shows very similar stress distributions for both plate types. However, the values in the extremes of the sample, that are in contact with the plates, are higher for the curved than for the flat plate.

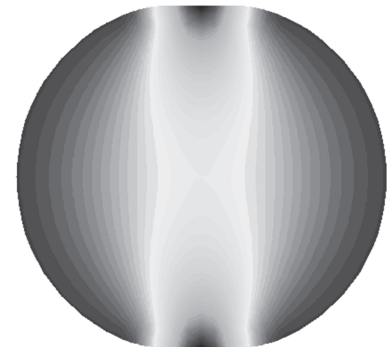
FLAC3D 3.00

Step 24000 Model Perspective
10:17:20 Wed Jun 05 2013

Center:	Rotation:
X: 0.000e+000	X: 0.000
Y: 1.250e-002	Y: 0.000
Z: 0.000e+000	Z: 0.000
Dist: 1.784e-001	Mag: 1
Increments:	Ang: 22.500
Move: 7.097e-003	Rot: 10.000

Contour of SZZ
Magfac = 1.000e+000
Gradient Calculation

-4.3302e+007 to -4.3000e+007
-4.1000e+007 to -4.0000e+007
-3.8000e+007 to -3.7000e+007
-3.5000e+007 to -3.4000e+007
-3.2000e+007 to -3.1000e+007
-2.9000e+007 to -2.8000e+007
-2.6000e+007 to -2.5000e+007
-2.3000e+007 to -2.2000e+007
-2.0000e+007 to -1.9000e+007
-1.7000e+007 to -1.6000e+007
-1.4000e+007 to -1.3000e+007
-1.1000e+007 to -1.0000e+007
-8.0000e+006 to -7.0000e+006
-5.0000e+006 to -4.0000e+006
-2.0000e+006 to -1.0000e+006
0.0000e+000 to 4.8481e+005



FLAC3D 3.00

Step 5000 Model Perspective
10:13:29 Wed Jun 05 2013

Center:	Rotation:
X: 0.000e+000	X: 0.000
Y: 1.250e-002	Y: 0.000
Z: 0.000e+000	Z: 0.000
Dist: 1.784e-001	Mag: 1
Increments:	Ang: 22.500
Move: 7.097e-003	Rot: 10.000

Contour of SZZ
Magfac = 1.000e+000
Gradient Calculation

-5.4901e+007 to -5.4000e+007
-5.1000e+007 to -5.0000e+007
-4.7000e+007 to -4.6000e+007
-4.3000e+007 to -4.2000e+007
-3.9000e+007 to -3.8000e+007
-3.5000e+007 to -3.4000e+007
-3.1000e+007 to -3.0000e+007
-2.7000e+007 to -2.6000e+007
-2.3000e+007 to -2.2000e+007
-1.9000e+007 to -1.8000e+007
-1.5000e+007 to -1.4000e+007
-1.1000e+007 to -1.0000e+007
-7.0000e+006 to -6.0000e+006
-3.0000e+006 to -2.0000e+006
1.0000e+006 to 2.0000e+006
4.0000e+006 to 4.2914e+006

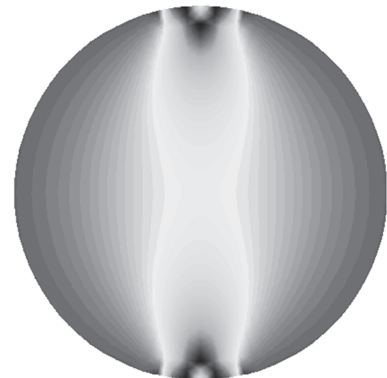


Figure 9. Vertical stress with flat (upper) and curved (lower) plates.
Source: Álvarez Fernández et al.

The same behavior was observed for a similar sample to that in Fig. 8 for vertical stresses (Fig. 9). Again, the curved plate shows higher stress values around plate-contact. However, the maximum point in this case is not in the extremes, as with the flat plate, but in its environment.

Tables 1 and 2 (flat and curved plates, respectively) report the numeric values obtained from the completed tests. They show Δr or radius shortening in mm due to deformation, α or deformation angle in sexagesimal degrees, and horizontal and vertical stress obtained by means of 3D numerical simulation (σ_{Fxx} , σ_{Fzz}) as well as through the application of the approximation developed by Hondros (σ_{Hxx} , σ_{Hzz}) (8). This is according to the load-application angle, which is considered equal to the deformation angle.

For low stiffness values below 13.5 GPa, the values of both horizontal and vertical stress, obtained in numerical simulation and flat plate (Table 1), are higher than those obtained with curved plate (Table 2). However, for stiffer samples, strengths do not depend on plate shape. The same occurs when stress is calculated with Hondros' approximation. However, in this case, low stiffness values give rise to higher stress with a curved plate, compared to with a flat plate; this is unlike what occurs with numerical simulation.

The value of horizontal and vertical stress calculated from Timoshenko's formulation (5) are 5.093 and 15.28 MPa,

respectively. Both values are slightly higher than the highest values obtained with both numerical simulation and Hondros' approximation.

Moreover, with stiffness values below 13.5GPa, increased sample stiffness leads to reduced sample deformation, thus giving rise to lower shortening and deformation angle values. In this case, the values obtained with flat plate are below those obtained with curved plate. However, for high stiffness values, deformation is similar regardless of plate shape.

Table 3 reports the values of average deviations among the strength values calculated with the three approximations that were considered. The lowest deviations for the flat plate occur between the strengths calculated according to Timoshenko's theory and those provided by the numerical simulation, while for the curved plate, the lowest deviations are observed with Hondros' approximation and the numerical simulation.

3 Conclusions

- Monitoring numerous tests allowed us to become more informed of sample behavior over time. Deformation is observed to cause surface sample-testing machine contact.

Table 1.
Numerical results of strengths for flat plates.

test	E (GPa)	Δr (mm)	α (°)	σ_{Fxx} (MPa)	σ_{Hxx} (MPa)	σ_{Fzz} (MPa)	σ_{Hzz} (MPa)
1	0.34	1.712	21.51	4.91	4.17	14.71	14.34
2	0.67	1.006	16.31	5.12	4.54	15.45	14.72
3	3.37	0.259	8.25	4.94	4.94	15.07	15.11
4	6.75	0.152	6.32	4.97	4.99	15.13	15.17
5	13.50	0.080	4.57	4.97	5.04	15.15	15.21
6	20.25	0.053	3.73	4.97	5.05	15.14	15.22
7	67.50	0.016	2.04	4.96	5.07	15.12	15.24

Source: Álvarez Fernández et al.

Table 2.
Numerical results of strengths for curved plates.

test	E (GPa)	Δr (mm)	α (°)	σ_{Fxx} (MPa)	σ_{Hxx} (MPa)	σ_{Fzz} (MPa)	σ_{Hzz} (MPa)
1	0.33	1.516	20.05	4.70	4.27	14.54	14.45
2	0.67	0.871	15.17	4.77	4.61	14.66	14.79
3	3.37	0.023	7.85	4.91	4.95	15.01	15.13
4	6.75	0.134	5.94	4.93	5.01	15.06	15.18
5	13.50	0.080	4.57	4.97	5.04	15.15	15.21
6	20.25	0.053	3.73	4.97	5.05	15.14	15.22
7	67.50	0.016	2.04	4.96	5.07	15.12	15.24

Source: Álvarez Fernández et al.

Table 3.
Average deviations between strengths values.

Plate	Horizontal strengths		
	Timoshenko - simulation	Hondros - Timoshenko	Hondros - simulation
flat	0.12	0.26	0.23
curved	0.21	0.23	0.14
Plate	Vertical strengths		
	Timoshenko - simulation	Hondros - Timoshenko	Hondros - simulation
flat	0.21	0.28	0.21
curved	0.32	0.25	0.10

Source: Álvarez Fernández et al.

- The deformation observed in samples causes sample lengthening along the OX axis and sample shortening along the OZ axis.
- The relationship between tensile and compressive stresses in numerical simulation has a theoretical value of around 3.
- Sample strengths and deformations depend on the sample material's stiffness.
 - Low stiffness values lead to large deformations and therefore greater vertical-axis shortening and greater deformation angles. Also, they give rise to lower strength values for both vertical and horizontal ones.
 - Conversely, stiffer materials show very small deformations, and have strength values approximate to the values obtained with Timoshenko's formulation, which do not depend on the sample's material.
- Strengths and deformations with flat plates are higher than those obtained with curved plates for materials with low stiffness values. However, for stiffness values over 13.5 GPa, plate shape has no impact on results.
- The strengths obtained according to Timoshenko theory are greater than those obtained by using numerical simulation.
- Finally, the strengths obtained from both 3D numeric simulation and Hondros' formulation in slightly deformed samples are lower than those obtained by using Timoshenko's formulation.

References

- Lizarazo-Marriaga, J.M. and Claisse, P., Compressive strength and rheology of environmentally-friendly binders. *Revista Ingeniería e Investigación*, 29(2), pp. 5-9, 2009.
- Valderrama, C.P., Torres-Agredo, J. and Mejía de Gutiérrez, R., A high unburned carbon fly ash concrete's performance characteristics. *Revista Ingeniería e Investigación*, 31(1), pp. 39-46, 2011.
- Mellor, M. and Hawkes, I., Measurement of tensile strength by diametral compression of discs and annuli. *Engineering Geology*, 5(3), pp. 173-225, 1971. DOI: 10.1016/0013-7952(71)90001-9
- SRM., Suggested methods for determining tensile strength of rock materials. *International Journal of Rock Mechanics and Mining Sciences Geomechanics Abstracts*, 1978, pp. 99-103.
- The Professional Standards Compilation Group of People's Republic of China. Specifications for rock tests in water conservancy and hydroelectric engineering (SLJ2-81). Beijing: China Waterpower Press, 1981.
- National Standards Compilation Group of People's Republic of China. Standard for tests methods of engineering rock masses (GB/T50266-99). Beijing: China Plan Press, 1999.
- The Professionals Standards Compilation Group of People's Republic of China. Specifications for rock tests in water conservancy and hydroelectric engineering (SL-264-2001). Beijing: China Waterpower Press, 2001.
- Hondros, G., The evaluation of Poisson's ratio and the modulus materials of a low tensile resistance by the Brazilian (indirect tensile) test with particular reference to concrete. *Australian Journal of Applied Science*, 10(3), pp. 243-268, 1959.
- Hudson, J.A., Brown, E.T. and Rummel, F., The controlled failure of rock disks and rings loaded in diametral compression. *International Journal of Rock Mechanics and Mining Science*, 9(2), pp. 241-248, 1972. DOI: 10.1016/0148-9062(73)90034-X
- García-Leiva, M.C., Ocaña, J., Martín-Meizoso, A. and Martínez-Esnaola, J.M., Fracture mechanics of sigma sml140+ fibre. *Engineering Mechanics*. 69(9), pp. 1007-1013, 2002. DOI: 10.1016/S0013-7944(01)00117-5

- [11] Fell, J.T. and Newton, J.M., Determination of tablet strength by the diametral compression test. *Journal of Pharmaceutical Sciences*, 39(5), pp. 688 - 691, 1970. DOI: 10.1002/jps.2600590523
- [12] Yu, Y., Question the validity of the Brazilian test for determining tensile strength of rock. *Chinese Journal of Rock Mechanical Engineering*, 24(7), pp.1150-1157, 2005. [in Chinese].
- [13] Timoshenko, S.P. and Goodier, J.N., *Theory of Elasticity*. 3rd Edition, Mc Graw-Hill, New York, 1970.
- [14] Yong, Y., Jianmin, Y. and Zouwu, Z., Shape effects in the Brazilian tensile strength test and a 3D FEM correction. *International Journal of Rock Mechanics and Mining Science*, 43(4), pp. 623-627, 2006. DOI: 10.1016/j.ijrmms.2005.09.005
- [15] Yong, Y., Jianxun, Z. and Jichun, Z., A modified Brazilian disk tension test *International Journal of Rock Mechanics and Mining Science*, 46(2), pp. 421-425, 2009. DOI: 10.1016/j.ijrmms.2008.04.008
- [16] Jonsen, P., Häggblad, H. and Sommer, K., Tensile strength and fracture energy of pressed metal powder by diametral compression test. *Powder Technology*, 176(2-3), pp. 148-155, 2007. DOI: 10.1016/j.powtec.2007.02.030
- [17] Jianhong, Y., Wu, F.Q. and Sun, J.Z., Estimation of the tensile elastic modulus using Brazilian disc by applying diametrically opposed concentrated loads. *International Journal of Rock Mechanics and Mining Science*, 46(3), pp. 568 - 576, 2008. DOI: 10.1016/j.ijrmms.2008.08.004
- [18] Es-Saheb, M.H., Albedah, A. and Benyahia, F., Diametral compression test: Validation using finite element analysis. *International Journal of Advanced Manufacturing Technology*, 57(5-8), pp. 501-509, 2011. DOI: 10.1007/s00170-011-3328-0
- [19] Frocht, M.M., *Photoelasticity*, Vol. 2, John Wiley & Sons Inc, New York, 1948.
- [20] UNE 22950-2. 1990., *Mechanical properties of rocks. Strength determination tests. Part 2: Tensile strength. Indirect determination (Brazilian test)*. Madrid: AENOR, 1990. 4 p.

M.I. Álvarez-Fernández, is a BSc. in Mining Engineering and Dr in Mining Engineering from the University of Oviedo, Spain. In 1997, she started her career as a lecturer at the University of Oviedo in the Department of Mining and Prospective Mines. Her teaching experience is focused on rock mechanics and soils, and mine design and monitoring. She has been a member of the Ground Engineering Research Group for more than 15 years. During this time she has collaborated on several European Projects and worked with prestigious companies in the mining and civil engineering fields. Over her professional career she has highlighted patents concessions and published many research papers in important international journals. ORCID: 0000-0002-5681-6530

C. González-Nicieza, is BSc. in Industrial and Mining Engineer from the University of Oviedo, Spain. After he received his PhD in Mining Studies, in 1986, he started working as a professor at the University of Oviedo (Dept. of Exploitation and Prospecting Mines). He focused on rock mechanics and soils, and mine design and monitoring. He has been the chief of the Ground Engineering research Group for more than 20 years and has collaborated on many European Projects. He has also worked with prestigious companies in the mining and civil engineering fields. Over her professional career she has highlighted patents concessions and published many research papers in important international journals. ORCID: 0000-0002-2575-9676

M.B. Prendes-Gero, received her PhD in Mining Studies in 2002. From 1997 she taught at the University of Oviedo in Spain, and has worked as a full professor since 2002. She is also an honorary visiting researcher at Sherbrooke University in Canada. She has published widely on genetic algorithms, on stability of roofs and on the mining area. She has received two research recognitions from the Spanish Government. Throughout her career she has coordinated a European Project and has been member of research groups in several projects at the Spanish National Research Program. In 2009 she was sub-director of the Polytechnic School of Mieres and she has participated in the elaboration of the new Mines studies at the European Space of Superior Education. ORCID: 0000-0001-9125-4863

J.R. García-Menéndez, is BSc. in Industrial Engineer. He has been a member of the Ground Engineering Research Group team of the University of Oviedo, Spain, since 1999. In this team he has collaborated on many projects for prestigious companies in the mining and civil engineering sectors. He has a wide experience in instrumentation applied to ground engineering (use, maintenance and repair) both in the laboratory and outside. ORCID: 0000-0001-9551-0617

J.C. Peñas-Espinosa, PhD in Mining Studies. He is the chief of OCA Constructions and Projects, an important enterprise in the civil engineering field. He has extensive experience in this sector due to the projects he has worked in throughout his career.

F.J. Suárez-Domínguez, received his PhD in Industrial Engineering studies in 1996. From 1994 he has taught at the University of Oviedo in Spain, working as a full professor since 2002. He has received two research recognitions from the Spanish Government. He has been member of research groups working on several projects at the Spanish National Research Program. He is also a member of the Research Group on Sustainable Construction, Simulation and Testing (GICONSIME). He has published 24 papers in national and international magazines. ORCID: 0000-0002-4630-1218



UNIVERSIDAD NACIONAL DE COLOMBIA

SEDE MEDELLÍN
FACULTAD DE MINAS

Área Curricular de Ingeniería
Geológica e Ingeniería de Minas y Metalurgia

Oferta de Posgrados

Especialización en Materiales y Procesos
Maestría en Ingeniería - Materiales y Procesos
Maestría en Ingeniería - Recursos Minerales
Doctorado en Ingeniería - Ciencia y Tecnología de
Materiales

Mayor información:

E-mail: acgeomina_med@unal.edu.co
Teléfono: (57-4) 425 53 68